FINAL REPORT

From

Proceedings of the Third Lunar Science Conference

Volume III

Title

Infrared and Raman Spectroscopic Studies of Structural Variations in Minerals from Apollo 11, 12, 14 and 15 Samples

P. A. ESTEP, J. J. KOVACH, P. WALDSTEIN and C. KARR, Jr.

Morgantown Energy Research Center
U. S. Department of the Interior
Bureau of Mines
Morgantown, West Virginia 26505

List of 10 key indexing words

Chromite
Clinopyroxenes
Glasses
Ilmenite
Olivine
Orthopyroxenes
Pyroxferroite
α-Quartz
Sanidine
Ülvospinel

[redacted]

D

OFFICE OF PRIME RESPONSIBILITY

Proceedings of the Third Lunar Science Conference

Volume III

Infrared and Raman Spectroscopic Studies of Structural Variations in Minerals from Apollo 11, 12, 14 and 15 Samples

P. A. ESTEP, J. J. KOVACH, P. WALDSTEIN and C. KARR, Jr.

Sample Numbers

10085,46

12018,26

12021,24

12070,24

14163,80

14259,15

14310,2

14310,93

14321,97

14321,108

15301,83

15601,72

INFRARED AND RAMAN SPECTROSCOPIC STUDIES OF STRUCTURAL VARIATIONS IN MINERALS FROM APOLLO 11, 12, 14 AND 15 SAMPLES

P. A. ESTEP, J. J. KOVACH, P. WALDSTEIN and C. KARR, Jr.

Morgantown Energy Research Center
U. S. Department of the Interior
Bureau of Mines
Morgantown, West Virginia 26505

3 Tables, 9 Figures

Reviews and proofs to:

Patricia A. Estep
Morgantown Energy Research Center
U. S. Department of the Interior
Bureau of Mines
P. O. Box 880
Collins Ferry Road
Morgantown, West Virginia 26505

Telephone:

(Office) 304/599-7282

(Home) 304/599-0663

OUTLINE

Abstract (small print)

INTRODUCTION

EXPERIMENTAL TECHNOLOGY (small print)

- A. Preparation of single grains for infrared and Raman spectroscopy
- B. Raman and infrared reflectance spectra of grains in polished rock samples

RESULTS AND DISCUSSION

- A. Structure determination of mineral grains
  - 1. Feldspars
    - a. Plagioclase
    - b. K-feldspar
  - 2. Pyroxenes
    - a. Orthopyroxenes
    - b. Clinopyroxenes
    - c. Pyroxenoids
  - 3. Olivines
  - 4. Opaque Oxides
- B. Bulk composition of composite lunar samples
  - 1. Basalt Grains and Sieved Fractions
  - 2. Glasses

Attached: 9 figures

3 tables (small print)

captions for figures (small print)

30 references (small print)

acknowledgments (small print)

Abstract

Infrared and Raman vibrational spectroscopic data, yielding direct information on molecular structure. have been obtained for single grains (>150 μm) of minerals, basalts and glasses isolated from Apollo 11, 12, 14 and 15 rock and dust samples, and for grains in Apollo 14 polished butt samples. From the vibrational data, specific cation substitutions were determined for the predominant silicate minerals of plagioclase (An_{71} to An_{95}), pyroxene (Fs_6 to Fs_{53}) and olivine (Fa_{14} to Fa_{45}). Unique spectral variations for grains of K-feldspar, orthopyroxene, pyroxenoid and ilmenite were observed to exceed the ranges of terrestrial samples, and these variations may be correlatable with formation histories. Alpha-quartz was isolated as pure single grains, in granitic grains composited with sanidine, and in unique grains that were intimately mixed with varying amounts of glass. Accessory minerals of chromite and ulvospinel were isolated as pure grains and structurally characterized from their distinctive infrared spectra. Fundamental vibrations of the SiO_4 tetrahedra in silicate minerals were used to classify bulk compositions in dust sieved fractions, basalt grains and glass particles, and to compare modal characteristics for maria, highland and rille samples. No hydrated minerals were found in any of the samples studied, indicating anhydrous formation conditions.

INTRODUCTION

Previously presented vibrational spectroscopic data for Apollo 11 and 12 samples (ESTEP et al, 1971) were obtained by macro-infrared methods, which required frequent grain combinations to obtain one milligram of sample for analysis. The application of microsampling techniques in the present work has eliminated the possibility of contamination from such combinations, has furnished new data on grain-to-grain structure variations, has made possible the identification of some trace accessory minerals and has made it possible to obtain infrared and Raman vibrational data on the same single grain. The improvement in sampling techniques thus necessitated an examination of mineral grains from some Apollo 11 and 12 samples that we previously studied, for an assessment of the technique and in order to compare grains with those from Apollo 14 and 15 samples. We found that single grain analyses on the Apollo 11 and 12 samples considerably broadened the compositional ranges for pyroxenes (Fs_{15}-Fs_{51}) and olivines (Fa_{26}-Fa_{38}), from the ranges previously obtained by grain-combination analyses.

The spectral data show both similarities and differences among the lunar maria, highland and rille samples that we studied in this work: three crystalline rocks (12018,26, 12021,24, 14310,93); six dusts (10085,46, 12070,24, 14163,80, 14259,15, 15301,83, 15601,72); one breccia (14321,108) and two potted butts (14310,2, 14321,97). We found that one of the Apollo 15 dusts (15301,83) had some mineral structural features (in ilmenite and bulk compositions) similar to those of highland samples, while these same features in the other Apollo 15 dust (15601,72) were more similar to those in maria samples. No hydrated minerals were found in any of the samples studied, indicating anhydrous formation conditions.

EXPERIMENTAL TECHNOLOGY

A. Preparation of single lunar grains for infrared and Raman spectroscopy

Single grains for analysis were isolated from the +100 mesh dry-sieved dust fractions and crushed rock fragments in a dry-nitrogen filled chamber. For a complete

mineral structure characterization, it was necessary to obtain both infrared and Raman spectra on the same individual grain. We therefore first obtained a Raman spectrum on a weighed grain, typically 400 - 200 μm, that was sealed under helium in a 0.5 mm diameter fused-quartz capillary (Uni-mex Company, Griffith, Indiana) to prevent sample oxidation by the laser beam in the Raman instrument. Raman spectra were obtained on a Spex Ramalog (Model 1401) spectrometer,[1] utilizing a Coherent Radiation argon-krypton (Model 52) laser source, and the Raman scattered light was observed at 90° to the incident beam. The laser beam could be focused to an area of 100 μm^2 for measurements on 150 μm diameter single grains. The thin-walled capillaries (10 μm) in which the samples were enclosed gave no interfering Raman lines when the laser beam was focused on the sample. After Raman data were obtained the grain was recovered and ground in air to a fine powder for infrared micro-sampling analysis, utilizing a specially designed microcrushing mortar, similar to the macro-crushing mortar previously described (ESTEP et al, 1971). Cesium iodide powder (Harshaw Chemical Company) was added directly to the preground sample in the mortar to give a sample concentration of approximately 0.33 weight percent. After blending, about 10 μg of this mixture was transferred to a Perkin-Elmer ultra-micro die to prepare a 1.5 mm diameter micropellet at 500 lb total load and under vacuum. Infrared pellets were scanned with a reflecting-type 6x ultra-micro beam condenser mounted on a Model 621 Perkin-Elmer grating spectrophotometer purged with dry air. Both infrared and Raman data were obtained as described on 40 selected grains from only Apollo 12 and 14 samples, while 570 individual grains were isolated and examined by infrared from all the lunar rock chips and dust samples.

B. Raman and infrared reflectance spectra of grains in polished rock samples

To obtain in situ and orientation information, infrared and Raman spectra of single grains were obtained directly from polished slabs of two Apollo 14 lunar rock samples. The laser-Raman beam was focused on selected grains embedded in the polished rock surface (under helium purge), by means of a specially designed aperture-mask device (MAKOVSKY, 1972), using masks with apertures of 0.5, 0.75, 1.0 and 1.5 mm diameters. Infrared specular reflectance spectra (13° angle of incidence) were subsequently obtained on the same selected grains (under dry air purge), utilizing a Perkin-Elmer micro-specular reflectance attachment on the infrared instrument, and masks with apertures that were 1.0 and 2.0 mm

---

[1] Equipment is named in this report for identification only and does not necessarily imply endorsement by the U. S. Bureau of Mines.

in diameter. To obtain bulk compositional information from the polished rock samples, similar to the infrared reflectance measurements made by PERRY et al (1972), we utilized a mask with a 5.0 mm diameter aperture. Techniques were developed for both Raman and infrared reflectance measurements that allowed good spectra to be obtained from pressed powders of terrestrial standards—a capability particularly necessary for obtaining data from powdered synthetic samples.

RESULTS AND DISCUSSION

A. Structure determination of mineral grains

The infrared spectral correlations previously developed for determining specific cation substitutions in the predominant silicate minerals of Apollo 11 and 12 samples (ESTEP et al, 1971) were applied to obtain a comparison with the Apollo 14 and 15 samples. These involved the use of determinative curves derived from studies on synthetic and terrestrial standards. The composition dependent infrared frequency shifts on which these curves were based allowed a determination of anorthite content in plagioclase feldspars, ferrosilite in pyroxenes and fayalite in olivines. It has recently been demonstrated that in Raman spectra, chain vibrations are sensitive to the population of the cation sites and reflect the crystal environment of the Si-O groups in a variety of silicate minerals (GRIFFITH, 1969). We observed composition dependent frequency shifts, specifically in Raman spectra of plagioclase, pyroxenes and olivines, and from these constructed determinative curves which provided information on the same cation substitutions as obtained from the infrared data. We obtained similar results with infrared reflectance and Raman spectra obtained directly on polished rock or pressed powder mineral samples. Data collected from studies on synthetic and terrestrial standards by these techniques also provided the same composition dependent frequency shifts which could be utilized to determine cation substitutions in the lunar silicate minerals.

Table 1 presents compositional data obtained for Apollo 11, 12, 14 and 15 silicate minerals. The table includes data only for single grains, whether isolated or measured in situ by Raman or infrared reflection techniques in the polished rock samples.

1. Feldspars

a. **Plagioclase** The abundant Apollo 14 and 15 plagioclase grains occurred in a wide range of morphologies and were predominantly calcium-rich (An_{71}-An_{95}). Compositions shown in Table 1 were derived from both infrared and Raman data, utilizing low-frequency absorption bands that are linearly dependent on calcium content (ESTEP et al, 1971).

b. **K-feldspars** From the Apollo 14 breccia we isolated seven white granular composite grains of K-feldspar and alpha-quartz with compositions ranging from predominantly K-feldspar to predominantly alpha-quartz. Such granitic components were reported in Apollo 12 breccias (SCLAR, 1971) (DRAKE et al, 1970, for rock 12013) and led to the suggestion that these constituents were derived from the lunar highlands where large masses of primary granitic rock could exist in addition to igneous rocks of gabbroic, noritic and anorthositic composition. Because these grains were recovered in small amounts from the Apollo 14 samples, it is still speculative as to whether such siliceous material represents any widespread geological formation on the lunar surface. Fig. 1 demonstrates the detection of alpha-quartz (curve a) and K-feldspar (curve b) in one of the granitic grains (curve c) in which these minerals are of approximately equal abundance. We further isolated five white granular grains of pure K-feldspar from the same Apollo 14 breccia. Isolation of these pure grains allowed a determination of the distribution of Al and Si cations over the tetrahedral lattice positions, which has been difficult to obtain from X-ray diffraction data because of the similarities of Al and Si X-ray scattering factors (BROWN, 1971). To quantify the varying degrees of disorder that are possible in K-feldspars, we applied the infrared method described by LAVES and HAFNER (1956), HAFNER and LAVES (1957) and BAHAT (1970), to a number of terrestrial samples of the three possible polymorphs, with examples of spectra shown in Fig. 2. In going from ordered microcline to orthoclase to disordered sanidine (curves a, b, c), a general band broadening can be observed, and the frequency of the absorption band A can be

seen to decrease from 642 to 632 cm^{-1} while that of band B increases from 529 to 543 cm^{-1}. The frequency difference between A and B can thus be used as an indication of relative degree of disorder in the feldspar lattice. Studies on the terrestrial samples show typical frequency difference decreases from 113 to 98 to 88 cm^{-1} in going from microcline to orthoclase to sanidine, respectively. Spectra of the lunar K-feldspar grains (for example, Fig. 2, curve d) showed AB frequency differences in the range of 93 - 83 cm^{-1}, indicating for some grains a lower degree of Al/Si ordering than that observed in any terrestrial sanidine samples, except for that from a submarine Hawaiian basalt (77 cm^{-1}) (ANDREWS, 1971). Since sanidine is the more stable polymorph above about 700° C, its identification in lunar breccia suggests processes on the lunar surface involving high temperatures. The lower degree of Al/Si ordering in the lunar breccia and Hawaiian basalt sanidines may indicate exposures to higher temperatures and/or more rapid quenching.

2. Pyroxenes

Seven different structural types of pyroxenes, characterized by their distinctive infrared spectra, were isolated from the lunar samples and these are listed in Table 1. Classification criteria were based on unique variations in band frequencies, resolution, splittings and relative intensities. Changes in these spectral parameters can be due to compositional variations (cation substitution), changes in crystal symmetry, or degree of order in the pyroxene lattice. Whereas phase designations derived by many other techniques are based on chemical composition, the vibrational data yields direct knowledge on structural states. Studies on terrestrial and synthetic pyroxene standards allowed a specific determination of the ferrosilite content and a semiquantitative determination of wollastonite content as shown in Table 1.

a. Orthopyroxenes Orthopyroxenes were isolated from the Apollo 11 dust and from all the Apollo 14 and 15 rock chips and dusts made available to us, as shown in Table 1. Specific ferrosilite contents for these were derived from a determinative curve prepared from 24 analyzed terrestrial samples of orthopyroxenes, for the

absorption band which shifts linearly from 400 to 350 cm^{-1} for Fs_5 to Fs_{88}. Fig. 3 shows the infrared spectral distinctions for grains of enstatite, bronzite and hypersthene orthopyroxenes isolated from the Apollo 14 breccia. In lunar enstatite spectra (curve a), a change in band structure in the region of the 400 cm^{-1} analytical band prevented a determination of ferrosilite content utilizing this band. The spectral changes (more fine structure) in the 500 - 400 cm^{-1} region were intermediate between those in orthoenstatite (from the Norton County achondrite, the Cumberland Falls achondrite and a synthetic from Tem-Pres Research Division, The Carborundum Co., State College, Pa.) and clinoenstatite (a natural sample from Cape Vogel, Australia, a Tem-Pres synthetic, and from the Bencubbin mesosiderite). The close comparison of breccia enstatite spectra with spectra of enstatite from these sources, and the fact that the changes did not occur in natural terrestrial magnesium-rich orthopyroxenes that we examined, suggest that the spectral changes may be the result of shock or high temperatures, rather than a simple composition effect. To obtain ferrosilite content for the breccia enstatite, we utilized the magnitude of the splitting in the Si-O stretching vibrations at 1064 and 854 cm^{-1} (Fs_6), which decreases regularly with increasing ferrosilite content as demonstrated in Fig. 3.

In a further comparison of lunar orthopyroxene spectra with those obtained from terrestrial metamorphic sources (HOWIE, 1963) (SADASHIVAIAH and SUBBARAYUDU. 1970), it was noted that a band at 450 - n^{-1} which was of medium intensity in spectra of the terrestrial samples, was considerably weaker in spectra of lunar grains with equivalent ferrosilite contents (Fig. 3 and 4). Further, the intensity of this absorption band in spectra of the terrestrial metamorphic orthopyroxenes can be seen in Fig. 4 to be dependent on ferrosilite content for compositions from Fs_{11} to Fs_{88}. Recent Mössbauer studies on terrestrial metamorphic orthopyroxenes (VIRGO and HAFNER, 1970) have shown that an increasing ferrosilite content produces a more disordered Fe^{2+} distribution over the nonequivalent octahedrally coordinated sites M1 and M2. Additional Mössbauer studies have further demonstrated

that this cation distribution is both temperature (VIRGO and HAFNER, 1969) (DUNDON and HAFNER, 1971) and shock dependent (DUNDON and HAFNER, 1971). We therefore examined samples of orthopyroxenes for which Mössbauer data is reported in an attempt to determine if the intensity of the 450 cm^{-1} band is related to this same structural variation. Fig. 5 demonstrates the effects of shock on the infrared spectrum of orthopyroxene from Bamle, Norway. Samples shocked to 250 kilobars, 450 kilobars and 1 megabar show a systematically decreasing intensity for the 450 cm^{-1} band and this correlates with the cation disordering detected by Mössbauer studies on these same samples (DUNDON and HAFNER, 1971). It can also be noted in Fig. 5 curve (d) that the 400 cm^{-1} analytical band nearly disappears with 1 megabar of shock, as observed in the breccia enstatite. We examined a sample of hypersthene (No. 115/30, Fig. 4, curve c) after it was heated to 1,000° C for 166 hours and rapidly quenched, and found a substantial decrease in the intensity of the 450 cm^{-1} band, correlating well with the cation disordering measured by Mössbauer studies on this same heated sample (VIRGO and HAFNER, 1969). We further observed the 450 cm^{-1} band to be considerably reduced in intensity in spectra of orthopyroxene grains that we isolated from several chondrites and mesosiderites, and in particular those from the Rose City and Farmington chondrites which have been shown to be cation disordered by Mössbauer studies (DUNDON and HAFNER, 1971) (DUNDON and WALTER, 1967). The correlation with Mössbauer data supports the interpretation that the intensity of this absorption band might be related to cation disorder in pyroxenes, rather than the lattice stacking disorder detectable by X-ray diffraction (POLLACK and DeCARLI, 1969). The 450 cm^{-1} absorption band appears in a frequency region typical for cation-oxygen stretching vibrations, bending vibrations of Si-O-Si groups in silicate chains, and lattice modes. It is expected that for any of these possible assignments, the distorted M2 octahedron would produce vibrational modes differing from those of the more regular M1 octahedron in the pyroxene structure. Thus, the reduced intensity of the 450 cm^{-1} band in spectra of the orthopyroxene grains that we isolated from the lunar samples and from meteorites

may indicate reduced occupancy of the preferred M2 sites, resulting from exposure to either high temperature or shock events. Spectra of orthopyroxene grains from the Apollo 14 breccia and dust 14259,15 exhibited a 450 cm^{-1} band relatively weaker than that in spectra of dust 10085,46, dust 14163,80, rock 14310,93 and the two Apollo 15 dusts, and this suggests differences in their formation histories. Further studies of this spectral variation in natural, heated and shocked samples could lead to estimates of specific temperatures and pressures, which in turn could be usefully applied in deducing sample history.

b. Clinopyroxenes The three distinctive clinopyroxene spectra that we obtained from the lunar samples are shown in Fig. 6. Systematic studies on four pyroxenes synthesized by Turnock, University of Manitoba, Canada (Wo_{20} with Fs_{14}, Fs_{40}, Fs_{56} and $Wo_{40}Fs_{30}En_{30}$) and eight pyroxenes synthesized by Tem-Pres Research (Wo_{10}, Wo_{20}, Wo_{30} and Wo_{40}, each with Fs_{22} and Fs_{45}) allowed us to assess the effects of calcium substitution on infrared spectra. As shown in Fig. 6, unique variations in band splittings of the Si-O stretching vibrations in the range 1060 - 850 cm^{-1} were observed, and the strong Si-O-Si bending vibration near 500 cm^{-1} shifts to lower frequencies, shows less fine structure, and splits as calcium increases. Specific ferrosilite contents for clinopyroxenes were determined from the same infrared analytical absorption band near 400 cm^{-1} as used for orthopyroxenes and for Apollo 11 and 12 clinopyroxenes (ESTEP et al, 1971). Because in iron rich augites (Fs_{40}) the 400 cm^{-1} analytical band splits and is weakened, an absorption band near 330 cm^{-1} (also varying regularly with ferrosilite content) was used to determine iron substitution. For both analytical bands we observed a general correlation of deepening pyroxene grain color with shifts to lower frequencies, as previously reported for Apollo 11 and 12 clinopyroxenes (ESTEP et al, 1971). The dark amber iron-rich augites (Fs_{45}-Fs_{53}) gave good spectral matches with ferroaugite ($Wo_{41}Fs_{51}En_{8}$) from the Skaergaard Intrusion of East Greenland (WILLIAMS et al, 1971). A Raman determinative curve for ferrosilite content in lunar pigeonites was derived by plotting the center of gravity of an intense doublet that shifted from 1014

to 1002 cm^{-1} as ferrosilite content varied from Fs_{15} to Fs_{60}. The curve exhibited an unusually abrupt frequency shift near $Fs_{33.5}$, suggesting a possible structural change at this composition where several Apollo 14 grains fell.

c. **Pyroxenoids** We isolated grains of pyroxenoids from rock 12021,24 and dust 15601,72 and used the infrared method described by LAZAREV and TENISHEVA (1961b) to confirm the pyroxmangite structure and to show that there are seven silicon tetrahedra repeat units in the silicate chains (Siebenerketten structure), as determined by BURNHAM (1971) for the pyroxferroite from an Apollo 11 rock. The method utilizes a series of absorption bands in the 750 - 550 cm^{-1} region (see Fig. 7), which correspond to that produced by a totally symmetric stretching vibration in SiO_4 tetrahedra. As coupling takes place to form chains, these split to give more absorption bands. Lazarev showed that there is a direct correspondence between the number of bands appearing in this region and the number of silicon-oxygen tetrahedra in the repeating unit of the silicate chain. He demonstrated, for example, that a structure with a repeat unit of seven tetrahedra indicates a chain of the type $[(SiO_3)_n]_\infty$ where n = 7. We applied Lazarev's correlations to the three synthetic pyroxenoids of Fig. 7 (curves a, b, e) and verified LIEBAU's (1956) general correlation that as the mean octahedral cation size decreases (Ca^{2+} to Fe^{2+}) the number of silicon tetrahedra in the repeat unit of the chain increases. For example, the composition of $Ca_{0.5}Fe_{0.5}SiO_3$ (curve a) shows three absorption bands in the 750 - 550 cm^{-1} region, indicating that n = 3 and verifying that this pyroxenoid has the bustamite structure. The synthetic pyroxenoid $Ca_{0.15}Fe_{0.85}SiO_3$ (curve b) showed seven absorption bands in the scale expanded spectrum of this same region, indicating the pyroxmangite structure. Similarly, scale expansion of the spectrum for $FeSiO_3$ (LINDSLEY et al, 1964) (curve e) shows the presence of eight absorption bands. Since Lazarev studied only structures for n = 2 to n = 7, a ninth absorption band may be out of the 750 - 550 cm^{-1} range in ferrosilite III, or may be accidently degenerate. Thus we presume that n = 9 for the composition $FeSiO_3$, in agreement with the Neunerketten chain configuration assigned by BURNHAM (1966) to this same sample. Spectra of the pyroxenoid

grains from both lunar samples (Fig. 7, curves c and d) were scale expanded in the region 750 - 550 cm^{-1} and a total of seven absorption bands could be counted in all spectra (as listed in Table 1), indicating the pyroxmangite structure with n = 7. All three grains from rock 12021,24 gave identical infrared spectra (for example, curve c) and corresponded closely with that of the synthetic sample $Ca_{0.15}Fe_{0.85}SiO_3$ (curve b), which is near the composition reported by WEILL (1971) for pyroxferroite from this rock. However, the spectrum of the pyroxenoid grain from dust 15601,72 (Fig. 7, curve d) showed shifts to lower frequencies for some absorption bands and more closely matched that of natural pyroxmangite ($Ca_{0.056}Mg_{0.054}Fe_{0.38}Mn_{0.51}SiO_3$) from Idaho (USNM 102794, HENDERSON, 1936). This spectral match, and the lighter color of the Apollo 15 grain suggest less iron in the pyroxmangite structure. These studies indicate that infrared spectroscopy could be applied in determining the compositional limits of the various pyroxenoid structures, which remain still largely unknown (BURNHAM, 1971).

3. Olivines

The olivine grains isolated in this work (Fa_{14}-Fa_{45}) were all in the forsterite-fayalite olivine series, and their spectra compared well with that previously published (ESTEP et al, 1971). For a given composition, lunar olivine spectra compared best with spectra of synthetic equivalents. Some grains from the Apollo 14 and 15 samples gave spectra of poor quality, showing a band broadening particularly in the region 1150 - 1000 cm^{-1}, suggesting a glass or silica association. In two grains (Fa_{41}) from dust 15301,83, alpha-quartz bands at 1075, 791 and 773 cm^{-1} were detected. Determinative curves for fayalite contents were used for an infrared absorption band which shifts linearly from 418 to 356 cm^{-1} for Fa_0 to Fa_{100}, and for a Raman doublet which shifts 865 - 845 cm^{-1} and 832 - 818 cm^{-1} for the same fayalite contents.

4. Opaque Oxides

Ilmenite grains were isolated as black lustrous grains from the maria, highland and rille samples listed in Table 2. Infrared spectra of some single grains showed weak Si-O

stretching frequencies in the range 1100 - 1000 cm^{-1}, suggesting silicate overgrowths. In spectra of terrestrial ilmenites from a variety of sources and with different formation histories, we have observed gradational frequency shifts for the predominant absorption bands, indicating subtle and continuously variable structural differences. To describe these variations, we have distinguished two end-members, Type I and Type II, according to the position of the lowest frequency absorption band for terrestrial samples. This diagnostic band varies, as seen in Fig. 8, from 305 cm^{-1} in Type I (curve b) to 275 cm^{-1} in Type II (curve d), and its frequency in spectra of all other terrestrial samples are intermediate between these two values. Spectra of lunar ilmenites similarly exhibited these same frequency variations and could be classified according to the terrestrial scheme, as shown in Table 2. There were both sample-to-sample spectral variations within the maria, highland and rille (Fig. 8, curves a and c) samples and grain-to-grain spectral variations within single samples. However, we observed a distinct general trend that absorption bands in the spectra of ilmenite from the highland samples and dust 15301,83 occurred at higher frequencies (closer to Type I) than those from the maria samples and dust 15601,72. The presumed shock histories of the samples showing the higher frequencies suggest that lattice disorder may be producing the spectral differences. As shown in Table 2, some ilmenite grains from the Apollo 14 and 15 samples showed frequencies higher (>305 cm^{-1}) and lower (<275 cm^{-1}) than those observed in any terrestrial sample.

From the groundmass of rock 12021,24 we isolated a single anhedral grain of a spinel-group mineral, with a black submetallic luster. Apollo 12 spinels have been shown to vary from chrome spinels to chrome ülvospinels (HAGGERTY and MEYER, 1970), which are members of the chromite ($FeCr_2O_4$) to ülvospinel (Fe_2TiO_4) continuous solid solution series. We compared the spectrum of the grain (Fig. 9, curve c) that we isolated with spectra of a series of 13 USGS standard chromite samples covering a wide range of elemental substitutions, and found that it matched best with sample No. 148005, shown as curve (b), Fig. 9. The composition for chromite No. 148005 closely approximates the range of compositions found for lunar chromites in Apollo samples by HAGGERTY and MEYER (1970), except for TiO_2.

The infrared spectrum of an opaque oxide grain isolated from dust 15601,72 (Fig. 9, curve e) can be seen to correspond better with that of synthetic ulvospinel (curve d) than with those of Al or Cr rich spinels (curves a and b), indicating a similar composition.

B. Bulk Composition of Composite Lunar Samples

1. Basalt Grains and Sieved Fractions

The frequency of the strong infrared Si-O stretching vibration near 1000 cm^{-1}, previously correlated with silica content (ESTEP et al, 1971), was used to compare spectra of basalt grains and sieved fractions from the lunar dusts and crushed rock chips. Spectra of basalt grains (1000 - 300 μm) isolated from the +100 mesh sieved fraction of the Apollo 14 samples (two dusts and a crushed breccia) and dust 15301,83, with Si-O frequencies ranging 1010 - 1000 cm^{-1}, indicate a predominance of plagioclase (1010 cm^{-1}) over pyroxene (980 cm^{-1}). Data from our infrared reflectance measurements also indicate a predominance of plagioclase (An_{90}) in the Apollo 14 samples, as ascertained from measurements of 20 mm^2 areas on the two polished butt samples. Absorption spectra of basalt grains from dust 15601,72, with Si-O stretching frequencies of 990 - 980 cm^{-1}, on the otherhand, showed a predominance of pyroxene and were more basic in composition, similar to the maria basalt grains previously studied. These same modal trends were observed in spectra of the -100 mesh sieved fractions of the dusts, obtained by using 200, 325 and 400 mesh screens. Spectra of the Apollo 14 dust sieved fractions (1005 - 1000 cm^{-1}) and dust 15301,83 sieved fractions (1000 cm^{-1}) showed a predominance of plagioclase, while spectra of dust 15601,72 fractions (980 cm^{-1}) showed a predominance of pyroxene, similar to the -100 mesh sieved fractions of the maria dusts previously studied. From the correlation plot relating Si-O stretching frequencies to silica content, the bulk compositions of all basaltic grains and sieved fractions (1010 - 980 cm^{-1}) from Apollo 14 and 15 samples were seen to be a basaltic range (54 - 42% SiO_2), as were those from the maria dusts (52 - 40% SiO_2).

2. Glasses

Overall infrared spectral characteristics of the glasses isolated from Apollo 14 and 15 samples, shown in Table 3, were similar to those from Apollo 11 and 12 samples, exhibiting three principal bands in the region of Si-O stretching, Si-O-Si stretching and Si-O-Si bending vibrations, near 1000 (s), 700 (w) and 460 (m) cm^{-1}, respectively. Raman spectra of glasses from Apollo 14 samples exhibited the same three principal absorption bands, with similar frequencies, band widths and relative intensities. Infrared spectra of many glass particles, both beads and irregular fragments, and in particular those of irregular fragments from dust 14259,15,showed fine structure characteristic of feldspars and pyroxenes, indicating partial devitrification or incomplete melting of these minerals. We estimated silica contents of the glasses from the same correlation plot as used for the basalt grains and sieved fractions. Compositions of true glasses from Apollo 14 samples (1010 - 980 cm^{-1}, 54 - 42 wt % SiO_2) were generally less basic than those from Apollo 15 (985 - 970 cm^{-1}, 44 - 38 wt % SiO_2), and probably reflect the higher feldspar and lower iron contents in the highland samples. In both infrared and Raman spectra of individual grains of Apollo 14 glasses and in the infrared spectra of Apollo 15 glasses we noted, as with Apollo 11 and 12 glasses, a general trend that as the frequency of the Si-O stretching vibration decreased, the frequency of the Si-O-Si bending vibration increased. We have not observed this trend in spectra of synthetic glasses or tektites, and the structural reason for this unique behavior has not yet been determined.

Several glass grains containing varying amounts of alpha-quartz were isolated from the three Apollo 11, 12 and 14 dusts listed in Table 3, and the distinctive infrared spectra of some of these grains matched well with those of glass grains (also containing quartz) that we isolated from the Stannern eucrite. Their identification in lunar dusts suggests that the quartz previously found in meteorites is not due to terrestrial contamination. In addition, the occurrence of these unique glass grains containing variable amounts of the low-temperature high-pressure phase of silica is geochemically significant. It suggests similar formation processes for grains in lunar dusts and eucrites, and supports the hypothesis of a similar origin (DUKE and SILVER, 1967).

ACKNOWLEDGEMENTS

We thank the following persons from this laboratory for aiding in the collection of infrared and Raman spectra: A. A. Angotti, R. C. Berkshire, Jr., E. E. Childers, B. D. Stewart, L. E. Makovsky, and W. H. Edwards. We are grateful to J. Dinnin, U. S. Geological Survey, for supplying analyzed chromite samples; to D. Virgo, Carnegie Institution of Washington, R. W. Dundon, Marquette University, and S. S. Hafner, University of Chicago, for samples of pyroxenes analyzed by Mössbauer spectroscopy; to E. Dowty, University of New Mexico, for samples of synthetic pyroxenoids synthesized by Lindsley and Dowty; to J. D. Stevens, Kennecott Copper Corporation, and R. J. P. Lyon, Stanford University, for supplying pellets and data for samples studied by Howie; to G. Kurat, Naturhistorisches Museum, Vienna, Austria, and E. J. Olsen, Chicago Natural History Museum, for meteorite samples; to M. Morgenstein, University of Hawaii, for samples of Hawaiian basalt; and to the following persons for supplying analyzed pyroxenes for our comparisons: R. A. Howie, University of London King's College, England, I. D. Muir, University of Cambridge, S. S. Ghose, University of California, G. M. Bancroft, University of Western Ontario, Canada, R. V. Fodor, University of New Mexico, J. S. White, Smithsonian Institution, G. V. Subbarayudu, State University of New York at Buffalo, and S. S. Pollack, Carnegie-Mellon University.

This research was sponsored by NASA under Contract No. T-1760A.

REFERENCES

ANDREWS J. E. (1971) Abyssal hills as evidence of transcurrent faulting on north Pacific fracture zones. Geol. Soc. Amer. Bull. 82, 463-470.

BAHAT D. (1970) Optical and infrared studies on high-temperature alkali feldspars. J. Geol. Soc. Aust. 17, 93-102.

BROWN G. E. (1971) Neutron diffraction of Al/Si ordering in sanidine. Geol. Soc. Amer., Abstracts of 1971 Annual Meeting 3 (7), 514.

BURNHAM C. W. (1966) Ferrosilite III: A triclinic pyroxenoid-type polymorph of ferrous metasilicate. Science 154, 513-516.

BURNHAM C. W. (1971) The crystal structure of pyroxferroite from Mare Tranquillitatis. Proc. Second Lunar Sci. Conf., Geochim. Cosmochim. Acta Suppl. 2, Vol. 1, pp. 47-57. MIT Press.

DRAKE M. J., McCALLUM I. S., McKAY G. M. and WEILL D. F. (1970) Mineralogy and petrology of Apollo 12 sample No. 12013: A progress report. Earth Planet. Sci. Lett. 9, 103-123.

DUKE M. B. and SILVER L. T. (1967) Petrology of eucrites, howardites and mesosiderites. Geochim. Cosmochim. Acta 31, 1637-1666.

DUNDON R. W. and HAFNER S. S. (1971) Cation disorder in shocked ortho-pyroxene. Science 174, 581-583.

DUNDON R. W. and WALTER L. S. (1967) Ferrous ion order-disorder in meteoritic pyroxenes and the metamorphic history of chondrites. Earth Planet. Sci. Lett. 2, 372-376.

ESTEP P. A., KOVACH J. J. and KARR C., Jr. (1971) Infrared vibrational spectroscopic studies of minerals from Apollo 11 and Apollo 12 lunar samples. Proc. Second Lunar Sci. Conf., Geochim. Acta Suppl. 2, Vol. 3, pp. 2137-2151. MIT Press.

GRIFFITH W. P. (1969) Raman spectroscopy of minerals. Nature 224, 264-266.

REFERENCES (Continued)

HAFNER S. and LAVES F. (1957) Order-disorder and infrared absorption. II. Variation in the position and intensity of certain absorption lines of feldspars on the structure of orthoclase and adularia. Z. Kristallogr. 109, 204-225.

HAGGFRTY S. E. and MEYER H. O. A. (1970) Apollo 12: Opaque oxides. Earth Planet. Sci. Lett. 9, 379-387.

HENDERSON E. P. and GLASS J. J. (1936) Pyroxmangite, new locality: Identity of sobralite and pyroxmangite. Amer. Mineral. 21, 273-294.

HOWIE R. A. (1963) Cell parameters of orthopyroxenes. Mineral. Soc. Amer. Spec. Paper 1, 213-222.

LAVES F and HAFNER S. (1956) Order-disorder and its effect on infrared absorption spectra. I. (Al, Si) Distribution in feldspars. Z. Kristallogr. 108, 52-63.

LAZAREV A. N. and TENISHEVA T. F. (1961b) Vibrational spectra of silicates. III. Infrared spectra of the pyroxenoids and other chain metasilicates. Optics and Spectros. (USSR) 11, 316-317.

LIEBAU F. (1956) Systematology of crystal structures of silicates with highly condensed anions. Z. Phys. Chem. 206, 73-92.

LINDSLEY D. H., DAVIS B. T. C. and MacGREGOR I. D. (1964) Ferrosilite ($FeSiO_3$): Synthesis at high pressures and temperatures. Science 144, 73-74.

LINDSLEY D. H. and BURNHAM C. W. (1970) Pyroxferroite: Stability and X-ray crystallography of synthetic $Ca_{0.15}Fe_{0.85}SiO_3$ pyroxenoid. Science 168, 364-367.

LYON R. J. P. (1963) Evaluation of infrared spectrophotometry for compositional analysis of lunar and planetary soils. Stanford Res. Inst., Final Rept. under contract NASr-49(04), Pub. by NASA as Tech. Note D-1871.

MAKOVSKY L. E. (1972) Sampling technique for Raman spectroscopy of minerals. In preparation.

REFERENCES (Continued)

PERRY C. H., AGRAWAL D. K., ANASTASSAKIS E., LOWNDES R. P., and TORNBERG N. E. (1972) Far infrared and Raman spectroscopic investigations of lunar materials from Apollo 11, 12, 14 and 15 (abstract). In Lunar Science - III (editor C. Watkins). pp. 605-607, Lunar Science Institute Contr. No. 88.

POLLACK S. S. and DeCARLI P. S. (1969) Enstatite: disorder produced by a megabar shock event. Science 165, 591-592.

SADASHIVAIAH M. S. and SUBBARAYUDU G. V. (1970) Orthopyroxenes from the Kondavidu charnockites, Guntur District, Andhra Pradesh. Proc. Indian Acad. Sci. 1970, 139-148.

SCLAR C. B. (1971) Shock-induced features of Apollo 12 microbreccias. Proc. Second Lunar Sci. Conf., Geochim. Cosmochim. Acta Suppl. 2, Vol. 1, pp. 817-832. MIT Press.

VIRGO D. and HAFNER S. S. (1969) Fe^{2+}, Mg order-disorder in heated orthopyroxenes. Mineral. Soc. Amer. Spec. Paper 2, 67-81.

VIRGO D. and HAFNER S. S. (1970) Fe^{2+}, Mg order-disorder in natural orthopyroxenes. Amer. Mineral. 55, 201-223.

WEILL D. F., GRIEVE R. A., McCALLUM I. S. and BOTTINGA Y. (1971) Mineralogy-petrology of lunar samples. Microprobe studies of samples 12021 and 12022; Viscosity of melts of selected lunar compositions. Geochim. Cosmochim. Acta Suppl. 2, Vol. 1, pp. 413-430. MIT Press.

WILLIAMS P. G. L., BANCROFT G. M., BOWN M. G. and TURNOCK A. C. (1971) Anomalous Mossbauer spectra of C2/c clinopyroxenes. Nature 230, 149-151.

Table 1. Compositional data for single grains of Apollo 11, 12, 14 and 15 silicate minerals

Mineral	Sample[1]	Description of mineral grains[2]	Number of analyses[3]	Analytical frequencies,[4] cm^{-1}	Derived composition
SILICA					
α-Quartz	10085,46	Black lustrous opaque, from a 2 mm conglomerate	1		
	12070,24	Mixed with glass; medium amber opaque	1		
	14259,15	Deep green, glossy, flat, 600 x 300 μm;	2	1075,791, 773,	
		Colorless transparent, 400 x 400 μm		454, 392, 368	
		Mixed with glass; light yellow to deep amber	17		
		transparent, yellow to green to brown opaque			
	14321,108	Composited with K-feldspar; white granular,	7		
		500 - 200 μm			
			1	467	
	15301,83	Mixed with olivine; medium yellow, honey	2		
		transparent			
	15601,72	Composited with other lunar silicates; black,	1		
		smooth surfaced, blocky			
FELDSPARS					
K-Feldspar	14321,108	White granular, 800 - 200 μm	5	638-631, 542-548	
		Composited with α-quartz; white granular,	7	637-625, 542-545	
		500 - 200 μm			
			1	516, 488	

(Table 1) (Estep)

Mineral	Sample	Description of mineral grains	Number of analyses	Analytical frequencies, cm^{-1}	Derived composition
Plagioclase	14163,80	Colorless transparent, white opaque, white granular	10	225 - 228	An_{79} - An_{85}
			2	507	> An_{90}
	14310,2	Collection of 200 μm colorless to grey transparent grains, 1200 x 1200 μm area	2	(560)	An_{95}
			2	508	> An_{90}
	14310,93	Colorless transparent	2	225, 230	An_{79}, An_{89}
	14259,15	Colorless transparent, tinted translucent, white opaque to colored opaque, white granular	20	225-230	An_{79} - An_{89}
	14321,97	Light grey transparent to chalky white, 1500 x 600 μm area	1	(565)	An_{90}
			7	508	> An_{90}
	14321,108	Colorless transparent, tinted translucent, white opaque	9	220 - 225	An_{71} - An_{79}
	15301,83	Colorless transparent, tinted translucent, white granular	9	225	An_{79}
	15601,72	Colorless transparent, white granular	7	225	An_{79}

(Table 1) (Estep)

Mineral	Sample	Description of mineral grains	Number of analyses	Analytical frequencies, cm^{-1}	Derived composition
PYROXENES					
Orthopyroxenes					
Enstatite	14321,108	Light yellow opaque	6	1060, 855	Fs_6 - Fs_{10}
			1	1018, 680, 668	n.d.[5]
Bronzite[6]	14321,108	Light yellow transparent	1	396	Fs_{11}
	15301,83	Light yellow opaque	2	396, 393	Fs_{11}, Fs_{16}
Bronzite-Hypersthene	10085,46	Medium amber transparent, from a 1.6 mm conglomerate	1	391	Fs_{19}
	14163,80	Yellow transparent	1	392	Fs_{17}
	14259,15	Light green opaque, light yellow opaque	2	395, 389	Fs_{13}, Fs_{22}
	14310,93	Light yellow transparent to translucent	5	393-392	Fs_{16} - Fs_{17}
	14321,97	Honey transparent, 600 x 600 μm area	1	(877)	Fs_{21}
	14321,108	Dark brown transparent	1	383	Fs_{32}
	15301,83	Light yellow transparent, light yellow to honey translucent	4	395 - 392	Fs_{13} - Fs_{17}
	15601,72	Light yellow transparent	1	390	Fs_{20}
Clinopyroxenes					
Pigeonite (Wo_5-Wo_{15})	12018,26	Yellow transparent	1	390	Fs_{24}
	12021,24	Yellow transparent	17	393 - 390	Fs_{20} - Fs_{24}
			1	1008, 676, 652	Fs_{33}
	12070,24	Honey transparent	2	390	Fs_{24}

(Table 1) (Estep)

Mineral	Sample	Description of mineral grains	Number of analyses	Analytical frequencies, cm^{-1}	Derived composition
Subcalcic augite (Wo_{15}-Wo_{25})	14259,15	Medium yellow transparent	1	390	Fs_{24}
	14310,93	Light yellow transparent	3	342 - 341	Fs_{9} - Fs_{11}
			1	1010, 682, 665	Fs_{30}
	14321,108	Honey transparent	3	385 - 383	Fs_{32} - Fs_{35}
	15301,83	Light yellow transparent	1	390	Fs_{24}
	15601,72	Medium yellow to medium amber transparent	5	393 - 380	Fs_{20} - Fs_{40}
	10085,46	Light and medium amber transparent, from a 2 mm conglomerate	2	388, 394	Fs_{27}, Fs_{18}
	12018,26	Light medium amber transparent	5	390 - 383	Fs_{24} - Fs_{35}
	12021,24	Light amber transparent	3	380	Fs_{40}
	12070,24	Honey to dark amber transparent	5	396 - 380	Fs_{15} - Fs_{40}
	14163,80	Light yellow transparent	1	392	Fs_{21}
	14259,15	Light amber translucent	1	380	Fs_{40}
			1	1013, 679, 663	Fs_{22}
	14321,97	Honey transparent	1	1004, 679, 663	n.d.
	14321,108	Honey to dark amber transparent	3	390 - 385	Fs_{24} - Fs_{32}
	15301,83	Golden yellow to medium amber transparent	3	387 - 375	Fs_{29} - Fs_{48}

(Table 1) (Estep)

Mineral	Sample	Description of mineral grains	Number of analyses	Analytical frequencies, cm^{-1}	Derived composition
Augite (Wo_{25}-Wo_{45})	15601,72	Honey to medium amber transparent	15	390 - 372	Fs_{24} - Fs_{53}
	10085,46	Medium to dark amber transparent, from a 2 mm conglomerate	9	390 - 385, 325 - 322	Fs_{24} - Fs_{32}, Fs_{35} - Fs_{41}
	12021,24	Medium to dark amber transparent	4	387 - 383, 322	Fs_{29} - Fs_{35}, Fs_{41}
	12070,24	Honey to reddish amber transparent	8	395 - 386, 325	Fs_{16} - Fs_{30}, Fs_{35}
	14259,15	Medium to reddish amber transparent	2	387	Fs_{29}
	15301,83	Light to dark amber transparent	5	387 - 383, 321 - 319	Fs_{29} - Fs_{35}, Fs_{43} - Fs_{46}
	15601,72	Yellow to dark amber transparent	8	394 - 385, 320 - 315	Fs_{18} - Fs_{32}, Fs_{44} - Fs_{53}
PYROXENOIDS	12021,24	Golden yellow transparent, subhedral equant, 500 - 300 μm	3	728, 705, 672, 660, 636, 575, 560	
	15601,72	Honey transparent, 400 x 400 μm	1	726, 705, 670, 659, 632, 572, 556	

(Table 1) (Estep)

Mineral	Sample	Description of mineral grains	Number of analyses	Analytical frequencies, cm^{-1}	Derived composition
OLIVINES	12070,24	Honey, opaque to transparent	4	402 - 394	Fa_{26} - Fa_{38}
	14163,80	Light yellow transparent	1	402	Fa_{26}
			1	855, 821	Fa_{27}
	14259,15	Light yellow to amber transparent, light yellow translucent	8	405 - 390	Fa_{22} - Fa_{45}
	14321,97	Gray translucent, with fractures, 1050 x 700 μ m area	1	850, 823	Fa_{40}
	14321,108	Light to dark yellow transparent, yellow to green opaque	15	410 - 390	Fa_{14} - Fa_{45}
		Light to medium yellow transparent	2	851, 819	Fa_{20}
	15301,83	Light yellow to honey, green, transparent to opaque; some rounded	21	402 - 390	Fa_{26} - Fa_{45}
	15601,72	Yellow to honey transparent, light yellow opaque	6	397 - 392	Fa_{34} - Fa_{41}

FOOTNOTES TO Table 1. **(Estep)**

[1] Lunar samples were classified as follows: 10085,46, fines to coarse fines; 12018,26, crystalline rock; 12021,24, crystalline rock; 12070,24, <1 mm contingency fines; 14163,80, <1 mm bulk fines; 14259,15, <1 mm comprehensive fines; 14310,2, potted butt of basaltic crystalline rock; 14310,93, basaltic crystalline rock; 14321,97, potted butt of coarse grained breccia; 14321,108, coarse grained breccia; 15301,83, <1 mm comprehensive fines; 15601,72, <1 mm comprehensive fines.

[2] Isolated single grains ranged 1500 - 150 μm and were typically 400 - 200 μm; single grains in polished samples examined by Raman and infrared reflectance techniques ranged 1500 - 200 μm.

[3] Number of grains isolated for infrared absorption analysis; number of areas examined by Raman and infrared reflectance techniques.

[4] Analytical Raman frequencies are underlined; infrared reflectance frequencies are in parentheses; only selected diagnostic frequencies are listed.

[5] n.d. = not determined.

[6] These unique bronzite grains (shown for example by Fig. 3, curve b) are listed separately from the other bronzites in this table because the Si-O stretching region pattern more closely matched pure enstatite (Fig. 3, curve a). All other bronzite grains isolated from the lunar samples more closely matched hypersthene (Fig. 3, curve c) in this spectral region.

Table 2. Single grains of ilmenite isolated from lunar rocks and dusts

Sample source	Sample type	Number of grains	Size, μm	Analytical frequency, cm^{-1}	Type classification[1]
10085,46	Dust, coarse fines	324[2]	100 avg.	285	Intermediate I - II
		10[3]	200 - 150	285 - 275	Intermediate I - II, Type II
12018,26	Crystalline rock	360[2]	100 avg.	290	Intermediate I - II
		3	150	290	Intermediate I - II
		2	200, 150	305	Type I
12021,24	Crystalline rock	349[2]	100 avg.	284	Intermediate I - II
		5	400 - 200	280 - 275	Intermediate I - II, Type II
14259,15	Dust	2	200, 150	310, 305	>Type I, Type I
14321,108	Breccia	6	300 - 150	305	Type I
		1	200	320	>Type I
15301,83	Dust	2	150	310	>Type I
15601,72	Dust	2	300, 400	280, 270	Intermediate I - II, <Type II

[1] For terrestrial ilmenites, Type I = 305 cm^{-1} and Type II = 275 cm^{-1} (see text); the closest type is underlined.

[2] These grains were combined for a single infrared macro-analysis (ESTEP et al, 1971), and are shown here for comparison. They were isolated from the −100 mesh sieved fractions of crushed fragments.

[3] Grains from a 2 mm and a 1.6 mm conglomerate.

Table 3. Glass grains isolated from lunar dusts

Sample source	Glass description[1]	Number analyzed	Frequencies, cm^{-1}	
			Si-O stretch	Si-O-Si bend
12070,24	Mixed with α-quartz; medium amber opaque	1	1000	458
14163,80	True glass; amber transparent, bead and fragment	2	1010, 990	462, 465
	Partially crystalline; light yellow to amber, green transparent fragments.	15	1020 - 980	462 - 488
14259,15	True glass; yellow to amber, green transparent, beads, fragments, vesicular and conglomerates.	11	1010 - 980	460 - 495
	Mixed with α-quartz; light yellow to dark amber transparent, yellow to green opaque, beads and fragments.	20	1020 - 980	458 - 472
	Partially crystalline; light yellow to green, amber transparent, beads and fragments.	29	1020 - 970	458 - 490
15301,83	True glass; green transparent, beads and fragments.	9	980 - 970	500 - 510
	Partially crystalline; yellow, green and amber transparent, beads and fragments.	14	1000 - 980	460 - 501
15601,72	True glass; dark amber transparent fragment, green transparent bead	2	985, 970	470, 500
	Partially crystalline; light yellow to green, brown transparent to opaque, beads and fragments.	4	990 - 980	475 - 500

[1] Size of beads ranged 800 - 200 μm; irregular fragments 1500 - 200 μm.

FIGURE CAPTIONS

Fig. 1 Infrared spectra of granitic constituents found in Apollo 14 samples. (a) α-quartz from dust 14259,15, 400 μm colorless transparent rounded grain, (b) sanidine from breccia 14321,108, 200 μm white granular grain, (c) granitic grain from breccia 14321,108, 200 μm white granular grain.

Fig. 2 Infrared spectra of K-feldspars. (a) microcline (Custer County, North Dakota), (b) orthoclase (Ray, Arizona), (c) sanidine (Drachenfels, Germany), (d) sanidine from breccia 14321,108, 200 μm white granular grain.

Fig. 3 Infrared spectra of orthopyroxenes from breccia 14321,108. (a) enstatite (Fs_6), 400 μm yellow opaque grain, (b) bronzite (Fs_{11}), 500 μm light yellow transparent grain, (c) hypersthene (Fs_{32}), 400 μm brown transparent grain.

Fig. 4 Infrared spectra of terrestrial metamorphic orthopyroxenes. (a) bronzite (Jackson County, North Dakota, USNM No. 47530), (b) bronzite (Madras, Howie No. 3709), (c) hypersthene (Virgo No. 115/30), (d) ferrohypersthene (Madras, Howie No. 137), (e) ferrohypersthene (Baffin Island, Howie No. 400), (f) eulite (Sudan, Howie No. 1002), (g) eulite (Virgo XYZ). Samples from HOWIE (1963) and VIRGO and HAFNER (1970). Spectra for Howie samples Nos. 3701, 137, 400 and 1002 were previously published by LYON (1963).

Fig. 5 Infrared spectra of orthopyroxene from Bamle, Norway (Fs_{24}). (a) natural, (b) shocked to 250 kilobars, (c) shocked to 450 kilobars, (d) shocked to 1 megabar.

Fig. 6 Infrared spectra of lunar clinopyroxenes. (a) pigeonite (Fs_{20}) phenocryst from rock 12021,24, 200 μm yellow transparent grain, (b) subcalcic augite (Fs_{15}) from dust 15301,83, 800 x 400 μm golden yellow transparent grain, (c) augite (Fs_{27}) from dust 15301,83, 200 μm light amber transparent grain.

FIGURE CAPTIONS (continued)

Fig. 7 Infrared spectra of pyroxenoids. (a) synthetic, $Ca_{0.50}Fe_{0.50}SiO_3$, (b) synthetic, $Ca_{0.15}Fe_{0.85}SiO_3$, (c) lunar, from rock 12021,24, 300 μm golden yellow transparent grain, (d) lunar, from dust 15601,72, 400 μm honey transparent grain, (e) synthetic, $FeSiO_3$ (ferrosilite III). (Synthetic samples synthesized by Lindsley and Dowty.)

Fig. 8 Infrared spectra of ilmenites. (a) lunar, from dust 15301,83, 100 μm black lustrous grain, (b) terrestrial, from Canada, Type I, (c) lunar, from dust 15601,72, 300 μm black lustrous grain, (d) terrestrial, from South Carolina, Type II.

Fig. 9 Infrared spectra of spinels. (a) synthetic hercynite ($FeAl_2O_4$), Tem-Pres Research, (b) chromite ($FeCr_2O_4$), Maryland (USGS No. 148005, 7.0% Al_2O_3, 52.2% Cr_2O_3, 27.6% FeO, 0.35% TiO_2, 9.9% MgO), (c) lunar chromite from rock 12021,24, 200 μm black grain, (d) synthetic ülvospinel (Fe_2TiO_4), Tem-Pres Research, (e) lunar ülvospinel from dust 15601,72, 200 μm black anhedral grain.

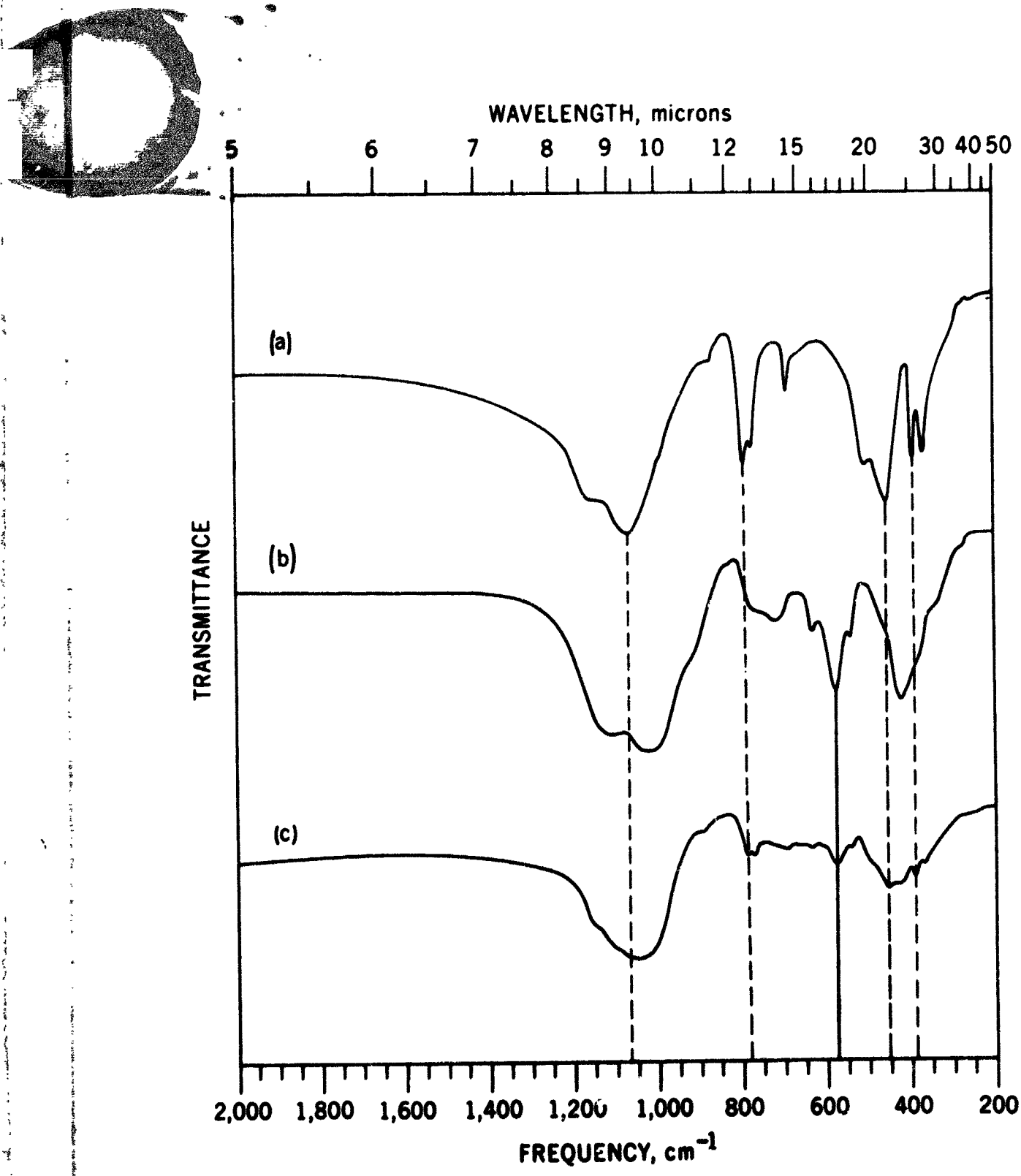
WAVELENGTH, microns
5
6
7
8
9
10
12
15
20
30
40
50
(a)
(b)
(c)
TRANSMITTANCE
2,000
1,800
1,600
1,400
1,200
1,000
800
600
400
200
FREQUENCY, cm⁻¹

Fig. 1

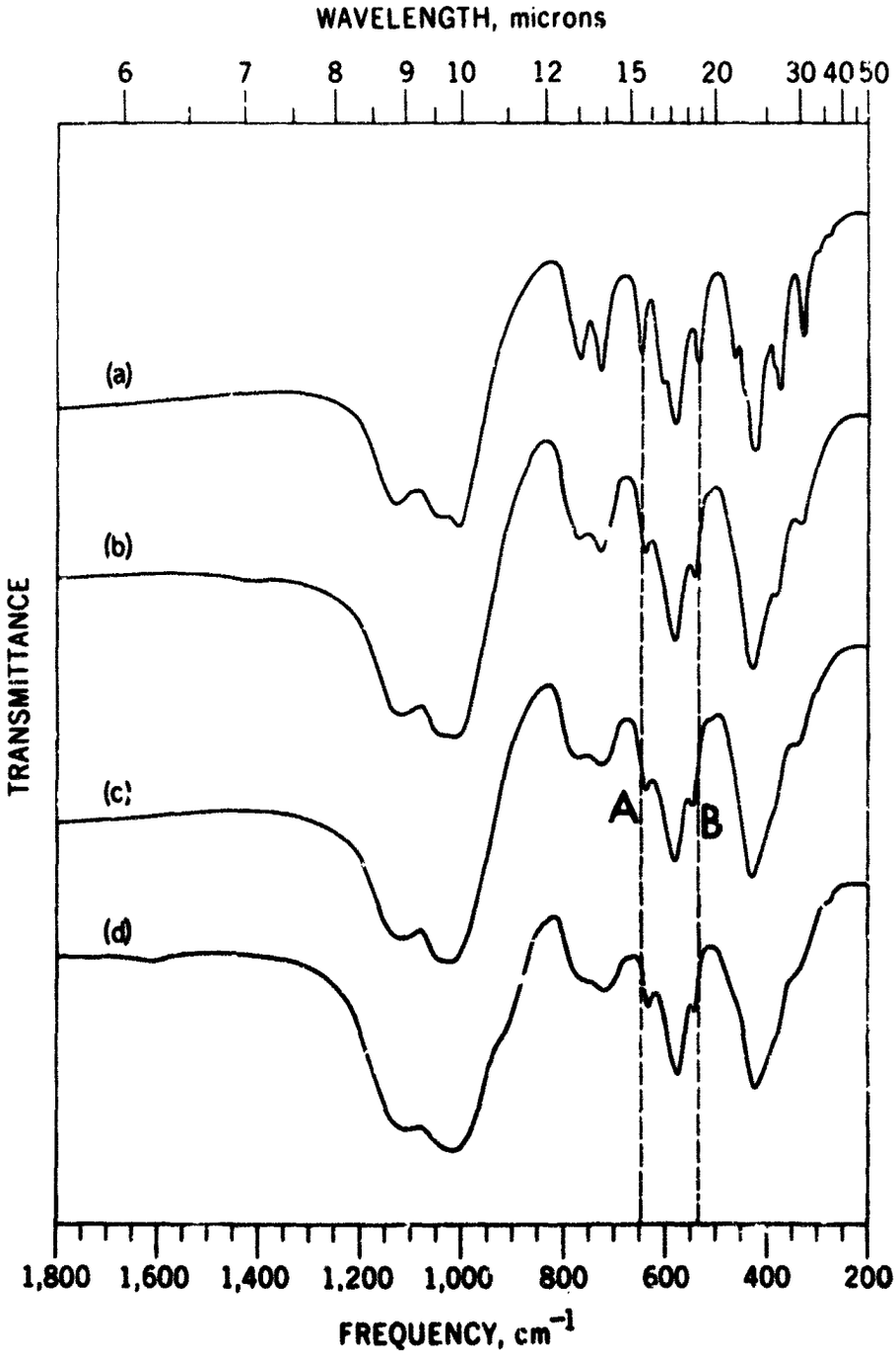
WAVELENGTH, microns
6
7
8
9
10
12
15
20
30
40
50
(a)
(b)
(c)
(d)
A
B
TRANSMITTANCE
1,800
1,600
1,400
1,200
1,000
800
600
400
200
FREQUENCY, cm^{-1}

Fig. 2

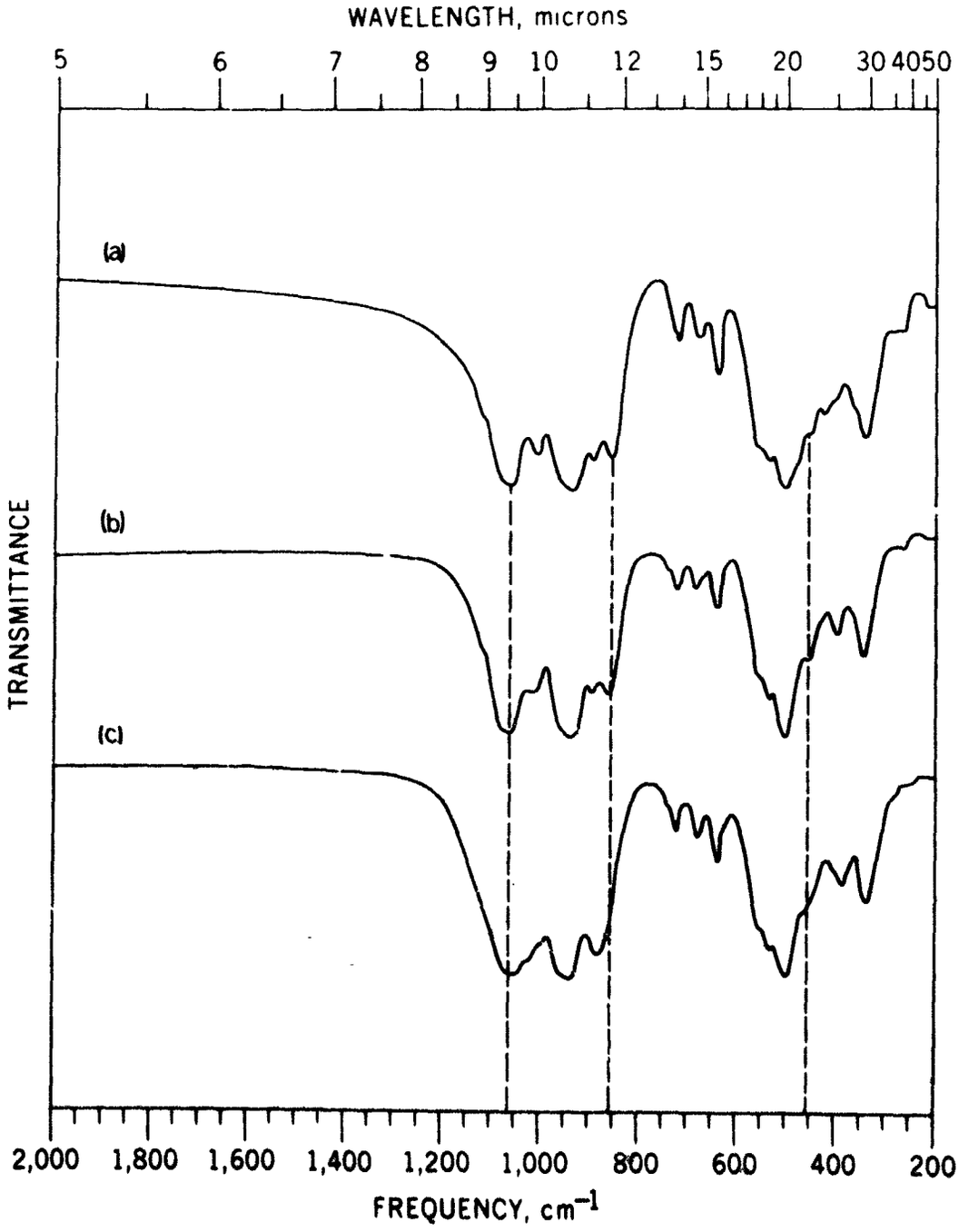
WAVELENGTH, microns
5
6
7
8
9
10
12
15
20
30
40
50
(a)
(b)
(c)
TRANSMITTANCE
2,000
1,800
1,600
1,400
1,200
1,000
800
600
400
200
FREQUENCY, cm^{-1}

Fig. 3

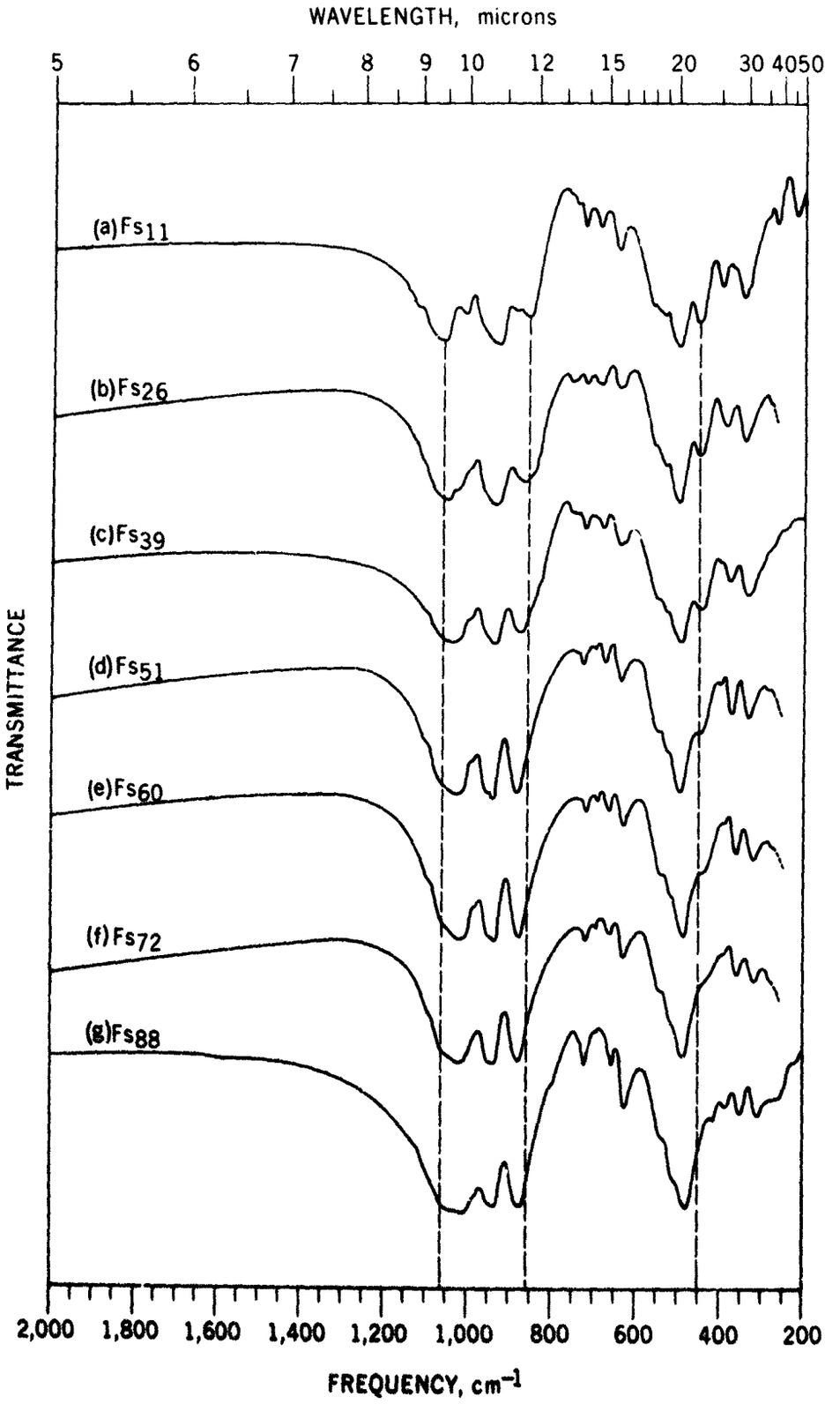
WAVELENGTH, microns
5
6
7
8
9
10
12
15
20
30
40
50
(a)Fs11
(b)Fs26
(c)Fs39
(d)Fs51
(e)Fs60
(f)Fs72
(g)Fs88
TRANSMITTANCE
2,000
1,800
1,600
1,400
1,200
1,000
800
600
400
200
FREQUENCY, cm-1

Fig. 4

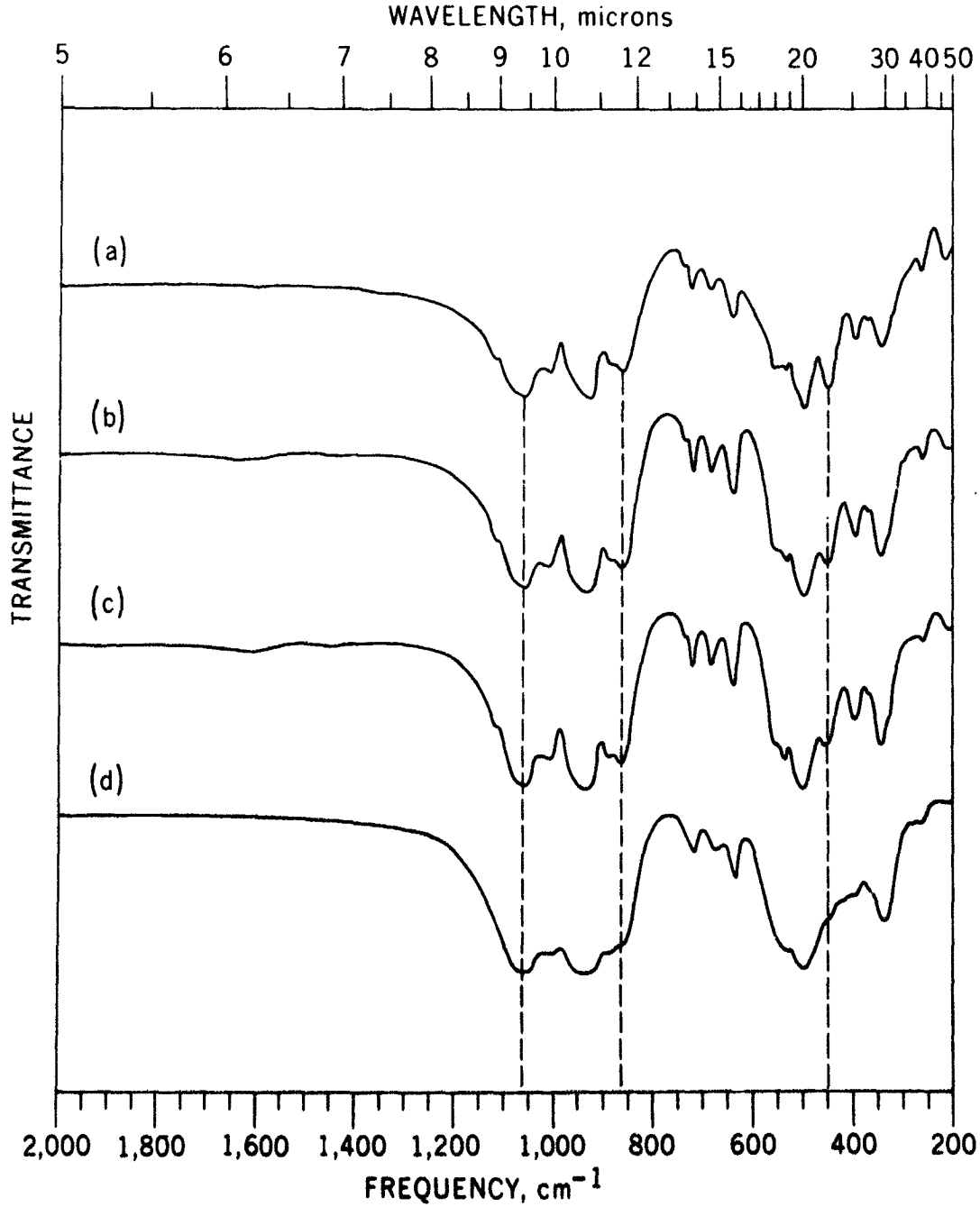
WAVELENGTH, microns
5
6
7
8
9
10
12
15
20
30
40
50
(a)
(b)
(c)
(d)
TRANSMITTANCE
2,000
1,800
1,600
1,400
1,200
1,000
800
600
400
200
FREQUENCY, cm⁻¹

Fig. 5

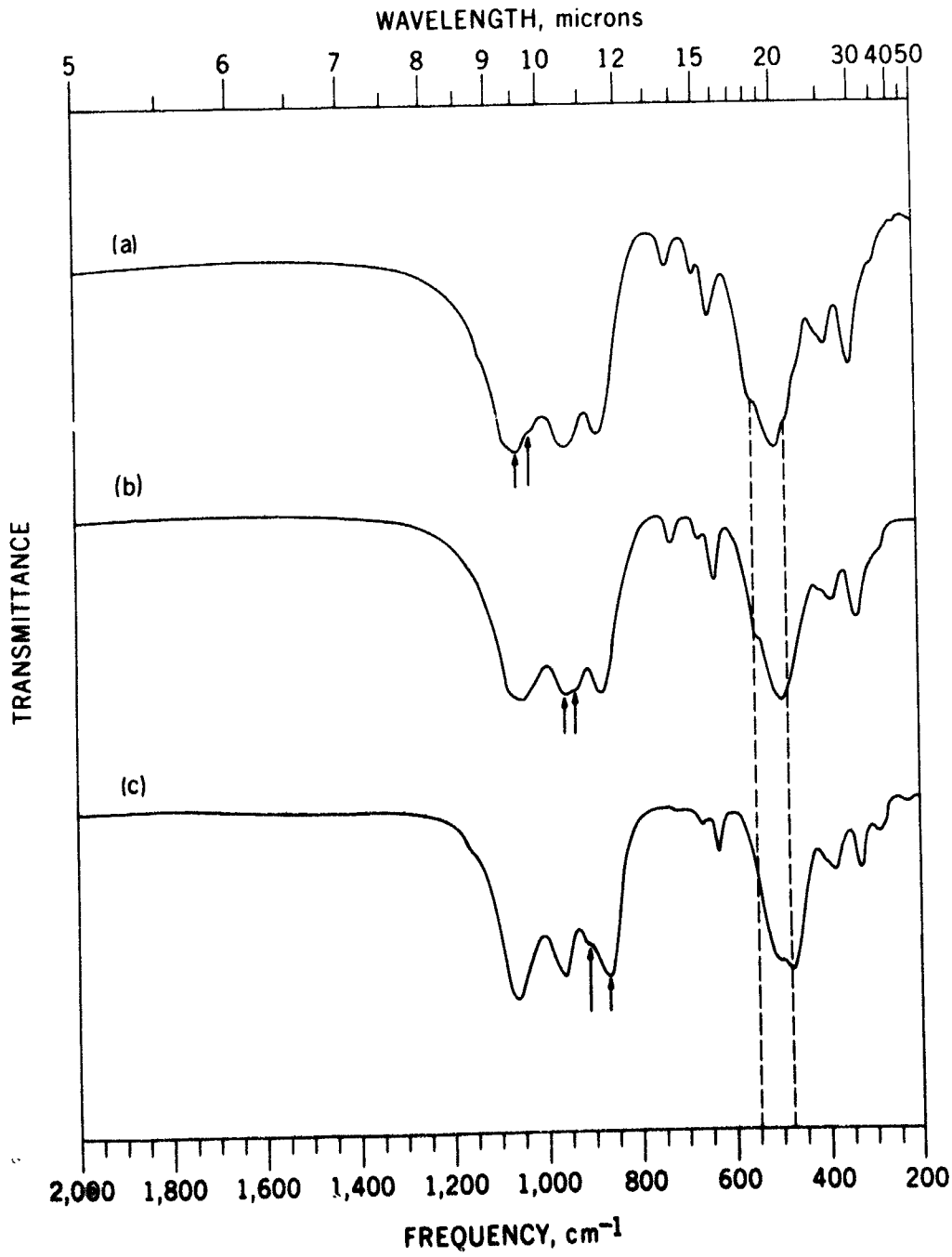
WAVELENGTH, microns
5
6
7
8
9
10
12
15
20
30
40
50
(a)
(b)
(c)
TRANSMITTANCE
2,000
1,800
1,600
1,400
1,200
1,000
800
600
400
200
FREQUENCY, cm⁻¹

Fig. 6

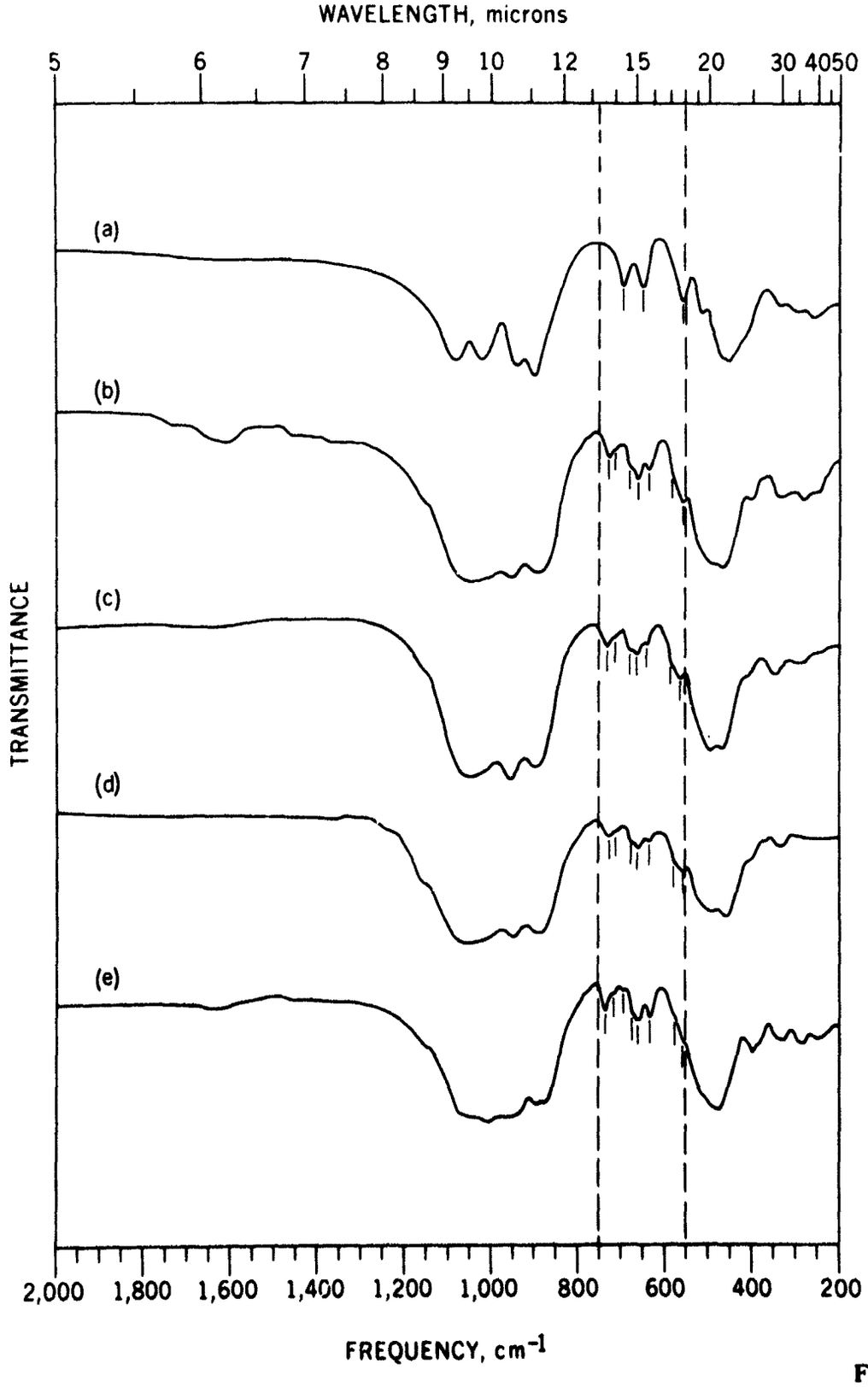
WAVELENGTH, microns
5
6
7
8
9
10
12
15
20
30
40
50
(a)
(b)
(c)
(d)
(e)
TRANSMITTANCE
2,000
1,800
1,600
1,400
1,200
1,000
800
600
400
200
FREQUENCY, cm-1

Fig. 7

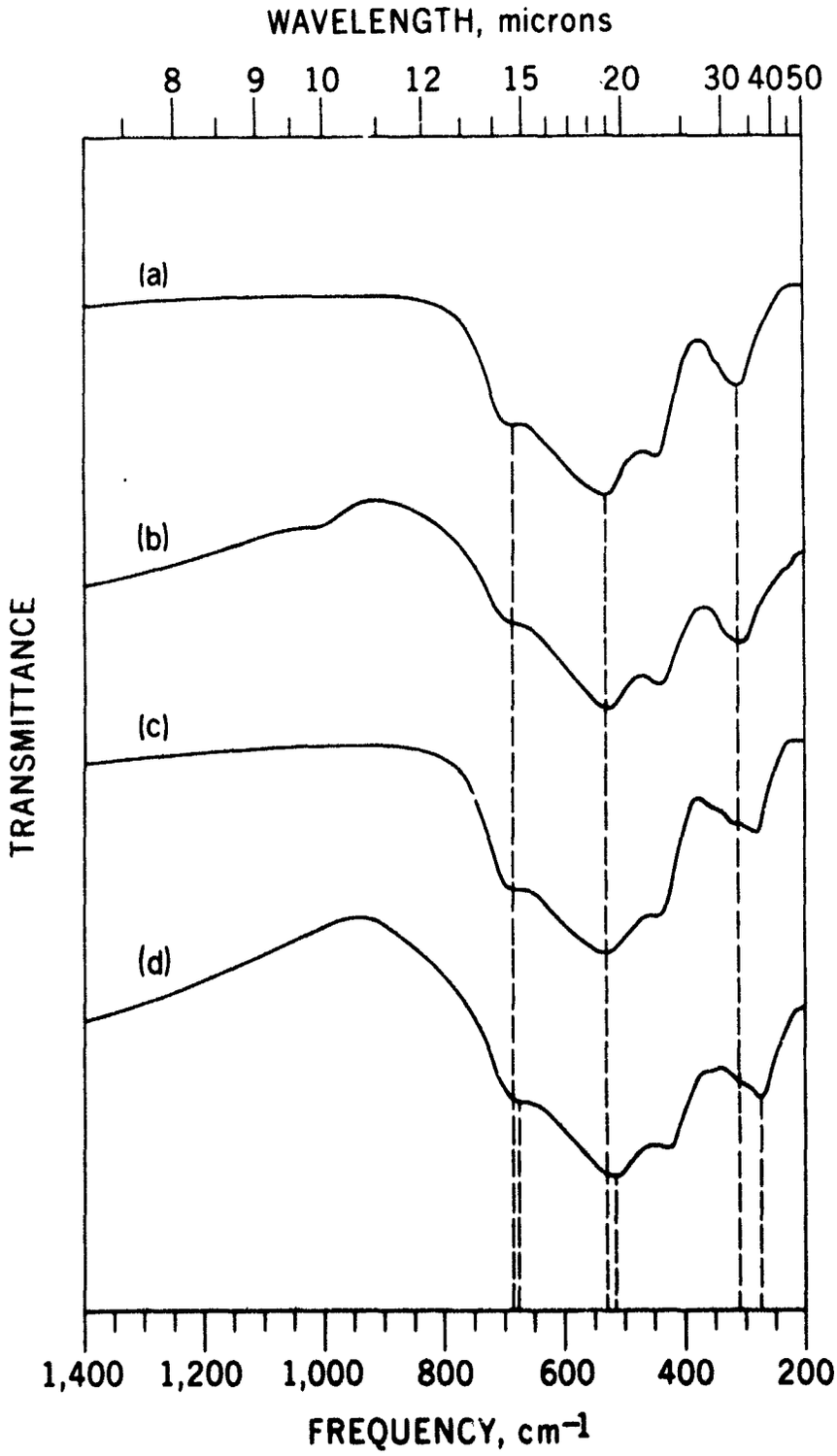
WAVELENGTH, microns
8
9
10
12
15
20
30
40
50
(a)
(b)
(c)
(d)
TRANSMITTANCE
1,400
1,200
1,000
800
600
400
200
FREQUENCY, cm⁻¹

Fig. 8

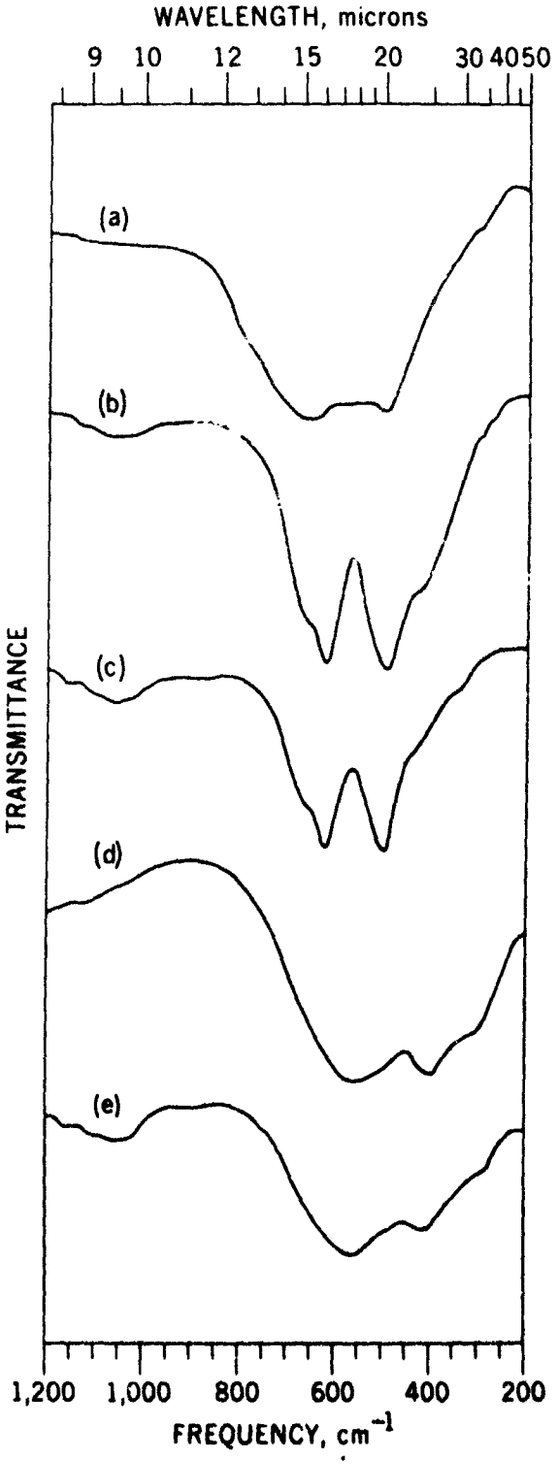
WAVELENGTH, microns
9
10
12
15
20
30
40
50
(a)
(b)
(c)
(d)
(e)
TRANSMITTANCE
1,200
1,000
800
600
400
200
FREQUENCY, cm^{-1}

Fig. 9